Turkish Journal of Physics

http://journals.tubitak.gov.tr/physics/

Research Article

Turk J Phys
(2021) 45: 159 – 168
© TÜBİTAK
doi:10.3906/fiz-2101-17

The investigation of the complex dielectric and electric modulus of Al/Mg_2Si/p-Si Schottky diode and its AC electrical conductivity in a wide frequency range

Ömer SEVGİLİ*
Vocational School of Health Services, Bingöl University, Bingöl, Turkey

Received: 30.01.2021 • **Accepted/Published Online:** 08.06.2021 • **Final Version:** 28.06.2021

Abstract: The Al/Mg_2Si/p-Si Schottky diode was fabricated using spin coating. The real (ε') and imaginary (ε'') components of complex dielectric (ε*), the real (M$'$) and imaginary (M$''$) components of complex electric modulus (M*) and AC electrical conductivity (σ_{AC}) of the fabricated Al/Mg_2Si/p-Si Schottky diode (SD) were examined by using the impedance spectroscopy (IS) measurements in a wide frequency range of 1 kHz-1 MHz. The ε' and ε'' were obtained using the value of measured capacitance and conductance while the values of dielectric loss tangent (tanδ, M$'$, M$''$ and σ_{AC} were obtained using the value of ε' and ε''. While the values of ε', ε'' and tanδ are almost independent of the frequency in the inversion and accumulation region, their value changes with the frequency, especially in the depletion region. The σ_{AC} was examined depending on the frequency and it was seen that its value increased with increasing frequency especially in depletion and accumulation region. The experimental results showed that the Mg_2Si can be used instead of conventionally used dielectric materials (SnO_2, SiO_2).

Key words: Dielectric properties, Al/Mg_2Si/p-Si Schottky diodes, complex dielectric permittivity and electric modulus, AC electrical conductivity, frequency-dependent

1. Introduction

The dielectric material is electrically insulating. Metal-oxide-semiconductor (MOS), metal-polymer-semiconductor (MPS) or metal-ferroelectric-semiconductor (MFS) structures can store charge thanks to the properties of the dielectric material used at the interface between metal and semiconductor. In these structures, charge storage depends on the thickness of the dielectric material and especially on the dielectric constant (ε') of the dielectric material. Such an interface layer separates the metal from the semiconductor and regulates the charge transitions. Additionally, the interfacial layer provides to realize the decrease in the magnitude of the leakage current, series resistance (R_s) values and interface states (N_{ss}) in the devices, it also increases the short circuit resistance (R_{sh}), barrier height and rectification ratio. In other words, such a layer affects the performance and reliability of the structure. Dielectrics materials are affected by an applied alternating electric field. By the formation of polarization in the material, it gains a dipole moment. By providing electrical charge accumulation on the dielectric surface, it exhibits capacitor behavior and can store charge [1–3]. The performance of semiconductor devices affects some factors such as the N_{ss}, R_s, the density of the interface states, temperature, frequency, voltage, and the form of the barrier between metal and semiconductor.

*Correspondence: omersevgili06@gmail.com

Magnesium silicide (Mg_2Si) is an intermetallic compound with relatively high melting temperature (=1085 °C), low density (=1.99 g/cm^3), a narrow-gap semiconductor (=0.6–0.7 eV), and a low thermal expansion coefficient (=7.5$\times 10^{--6}$ K) [4–6]. Its conduction types are p-type and it has been widely used as a semiconductor and thermoelectric material [6–10]. Mg_2Si is one of the attractive materials for optoelectronic application [11–13]. Additionally, researchers mostly focused on ceramic materials such as $MgSiN_2$ and $Mg_2Si_{(1-x)}V_xO_4$ [14, 15].For instance; according to Lenčéš et al. [14], the relative dielectric constant for $MgSiN_2$ powder obtained from a mixture of Mg_2Si is 9.0 at 100 kHz.

The research on the dielectric properties of Mg_2Si has been limited in the literature. Additionally, the change in frequency has a significant effect on the dielectric properties of structures that can store charge. Thus, in this study, the frequency-dependent properties of $\varepsilon\prime$, $\varepsilon\prime\prime$, tanδ M$\prime$, M$\prime\prime$ and σ_{AC} for Al/Mg_2Si/p-Si SD were examined by using the admittance measurements including measured capacitance and conductance data in a wide frequency range from 1 kHz to 1 MHz, and detailed.

2. Materials and methods

The wafer (p-Si) with boron-doped p-Si with 1–10 Ω cm resistivity, approximately 525 μm thickness and (**??**) orientation was chemically cleaned using acetone (C_3H_6O), isopropanol (C_3H_8O), and deionized (DI) water for 5 min, respectively. To remove the native oxide layer on the surface of the wafer was washed with HF. The wafer was washed again with DI for 5 min and dried with nitrogen. For omic contact, Al was coated on the back of the wafer in thermal evaporation. For a low resistance, the Al metal was precipitated into the semiconductor by annealing at 450 °C in N_2 environment for 5 min. A mixture of 1 mL of chloroform and 50 mg of Mg_2Si in powder form was thoroughly mixed with the aid of a centrifuge and synthesis of the interface layer was completed. Then, the interface layer was covered by spin-coating on the front of the wafer. To form rectifier (Schottky) contacts with 0.5 mm radius, Al was evaporated on the interface-covered surface and Al/Mg_2Si/p-Si SD was fabricated. Frequency-dependent capacitance (C) and conductance (G/ω) measurements of Al/Mg_2Si/p-Si SD were performed by using HP4192A impedance analyzer. Figure 1 shows the capacitance and conductance measuring system and the cross section of Al/Mg_2Si/p-Si SD.

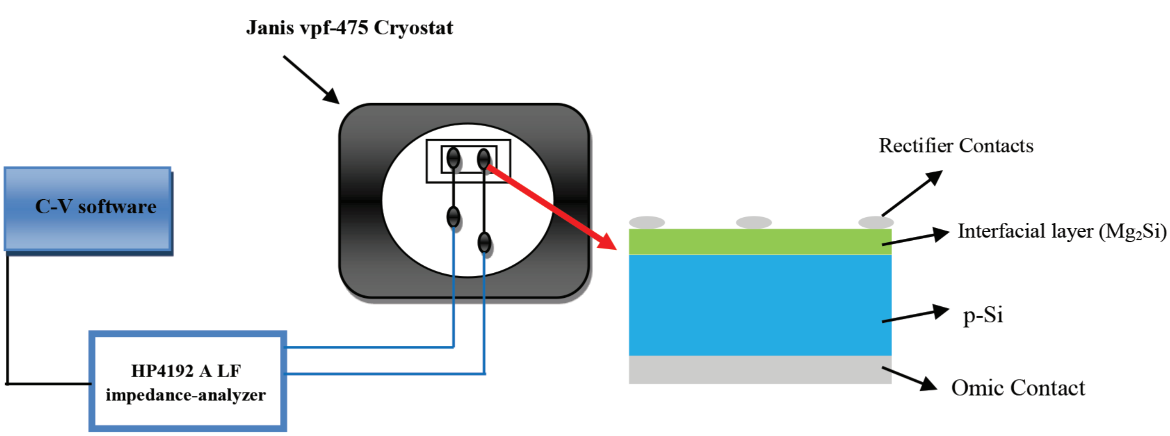

Figure 1. The capacitance and conductance measuring system and the cross section of Al/Mg_2Si/p-Si SD.

3. Results

The equivalent circuit for Al/Mg_2Si/p-Si SD is shown in Figure 2. As can be seen from Figure 2, the equivalent circuit consists of the total series resistance (R_s), a parallel junction capacitance (C) and the shunt resistance (R_{sh}), where C and R_{sh} are connected in parallel while R_s is connected in series to both C and R_{sh} [16,17].

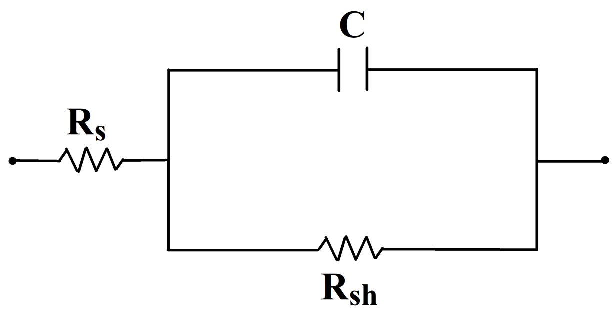

Figure 2. The equivalent electrical circuit for Al/Mg_2Si/p-Si SD.

Metal/semiconductor contacts behave like a parallel plate capacitor. In the presence of an insulating or organic interface layer, a capacitance (C) is formed between the metal and the semiconductor. The relationship of this capacitance and the capacitance of the interface layer (C_{ox}) and the capacitance of the semiconductor (C_{sc}) is given as follows [17,18]:

$$\frac{1}{C} = \frac{1}{C_{oc}} + \frac{1}{C_{sc}}. \tag{1}$$

The capacitance (C) and conductance (G) measurements for Al/Mg_2Si/p-Si SD are carried out in a wide range of frequencies (1 kHz–1 MHz). The dielectric properties of the structures are examined using these measurements. The ε^* of a structure provides information on its ε' and ε''. Thus, ε^* is given as follows [19,20]:

$$\varepsilon^* = \varepsilon' - j\varepsilon'' = \left(\frac{C_m d_i}{\varepsilon_0 A}\right) - j\left(\frac{G_m d_i}{\varepsilon_0 A}\right), \tag{2}$$

where ε',ε'', C_m, G_m, d_i, A and ε_0 are the real part and the imaginary part of complex dielectric permittivity, measured capacitance, measured conductance, the interfacial layer thickness, the area of the diode and the permittivity of vacuum, respectively [21–24]. ε' is the maximum value of the energy stored in the dielectric material under the external electric field and it depends on some physical and chemical factors such as frequency, defects of dielectric materials and the chemical structure [2,25,26]. ε'' is the energy loss caused by the slow polarization currents and the orientation of molecular dipoles in the dielectric material under the external electric field [26]. Briefly, ε' represents the charging while ε'' represents the loss current. The ε'-V and ε''-V plots for the Al/Mg_2Si/p-Si SD were given in Figures 3 and 4, respectively. The ε'-V and ε''-V plots have regions of inversion, depletion, and accumulation for each frequency. As shown in Figure 3, ε' was taken an almost constant value in the inversion and accumulation region and it increases with decreasing frequency in the depletion region. The space charges have not enough time to orient themselves in the direction of the alternating field at high frequencies. However, they have enough time for orientation at low frequencies. Hence, dielectric constant increases due to such behavior of space charges at low frequencies [27–32].

The ε'' value of Al/Mg_2Si/p-Si SD behaves just like ε' in the inversion and accumulation region. Especially at low frequencies, the high values of ε' and ε' are higher than their high-frequency values due to

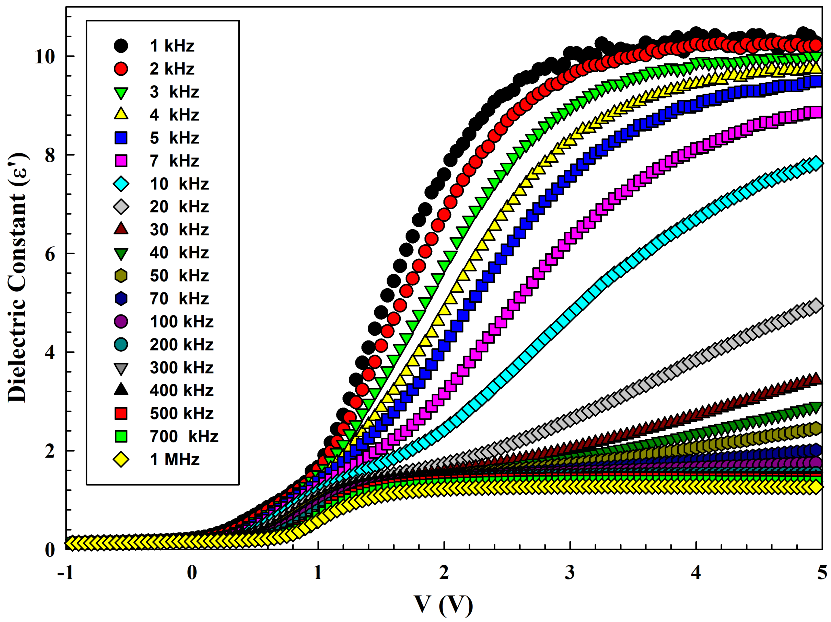

Figure 3. ε'-V plot for Al/Mg_2Si/p-Si SD in a wide frequency range.

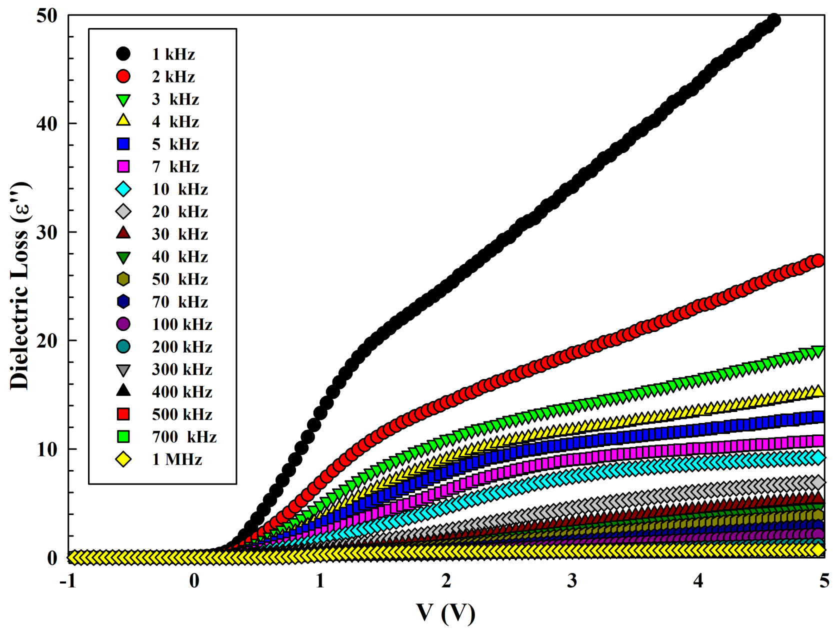

Figure 4. ε''-V plot for Al/Mg_2Si/p-Si SD in a wide frequency range.

interfacial polarization. The distributions in ε' and ε'' with frequency may be caused by electronic and ionic polarization effective at high frequencies (f $\geq 10^9$ Hz) and bipolar and surface polarizations that are effective at low frequencies (f $\leq 10^3$ Hz). Also, the correlation of ε' and ε'' with frequency is related to the capacitance and conductance values. Additionally, while the existence of N_{ss}, which can follow the alternating signal at low or intermediate frequencies, contributes to the capacitance and conductivity values in depletion and inversion regions, R_s is effective in the accumulation region.

The $\tan\delta$, indicating the energy loss of the structure during AC current conduction, is a measure of the ratio of electrical energy loss to stored energy at applied bias voltage and is given as follows [33]:

$$\tan\delta = \frac{\varepsilon''}{\varepsilon'}. \tag{3}$$

$\tan\delta$ depends on interface polarization and dipole orientations [34]. The $\tan\delta$-V plot for Al/Mg_2Si/p-Si SD was given in Figure 5. As shown in Figure 5, it was taken an almost constant value in the inversion and accumulation region. However, it has apronounced and sharp peak that arises from the N_{ss} at low frequencies. The peak behavior of the $\tan\delta$-V has occurred especially in the depletion region between ∼0 V and ∼2 V. Such phenomena of $\tan\delta$ are due to a particular distribution of charges and interfacial polarization mechanism, the density of the N_{ss} and the thickness of the interface layer (Mg_2Si) [3, 25]. Additionally, the peak value loses its effect with increasing frequency since charge carrier hopping cannot follow the external signal in high frequency. This indicates a relationship between dielectric behavior and conduction mechanisms of the diode.

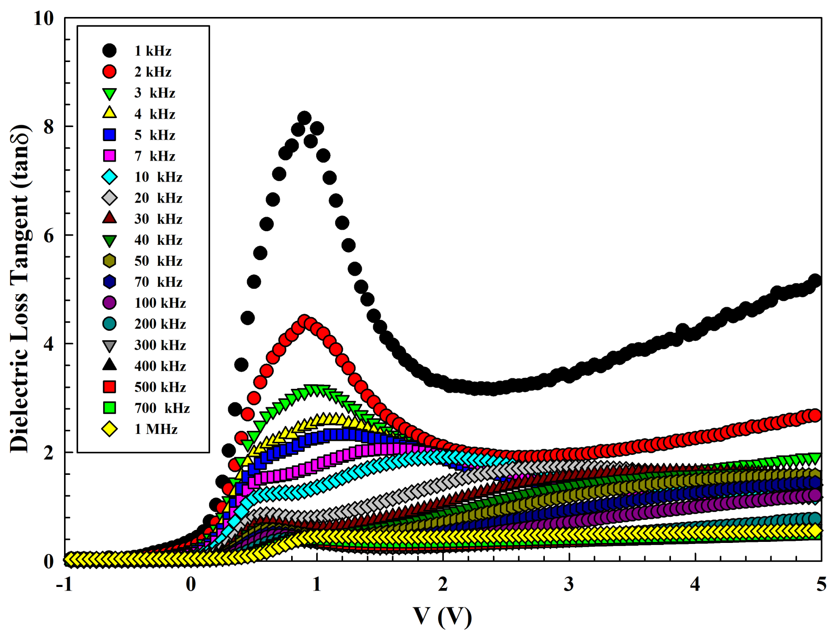

Figure 5. $\tan\delta$-V plot for Al/Mg_2Si/p-Si SD in a wide frequency range.

Physically, the complex electric modulus (M*) is used to understanding the dielectric relaxation process of the material. M* provides information about polarization mechanisms in the material and electrical transport process parameters such as carrier hopping rate and conductivity relaxation time. M* is calculated using ε' and ε" and is given as follows [35, 36]:

$$M^* = \frac{1}{\varepsilon^*} = M' + jM'' = \left(\frac{\varepsilon'}{(\varepsilon')^2 + (\varepsilon'')^2}\right) + j\left(\frac{\varepsilon''}{(\varepsilon')^2 + (\varepsilon'')^2}\right), \tag{4}$$

where M′ and M′′ the real and the imaginary part of M*, respectively. Thus, M′-V and M′′-V plots for the Al/Mg_2Si/p-Si SD were given in Figures 6 and 7, respectively. As shown in Figure 5, the M′ is independent of frequency in the accumulation region. The M′ value reaches its maximum value at high frequencies since the dielectric relaxation mechanisms depend on frequency [37]. As seen in Figure 7, while M′′ is independent of frequency in the inversion and accumulation region, it has a peak of different magnitude for all frequencies in the depletion region. M′′ reaches the maximum value in high frequency. The peak is shifting to the accumulation region with increasing frequency and its magnitude decreases. This situation is due to the Maxwell–Wagner type (MWt) interface polarization and the distribution of N_{ss} ingrained at the junction of the interfacial layer (the Mg_2Si) and the semiconductor (p-Si) [38,39]. The charges placed in N_{ss} affect both the electrical and dielectric properties. Because these traps or permitted energy levels can both hold and release some loads under an electric field or applied bias voltage. Most types of N_{ss} that have different lifetimes can be used at low frequencies because they can catch up with the ac signal.

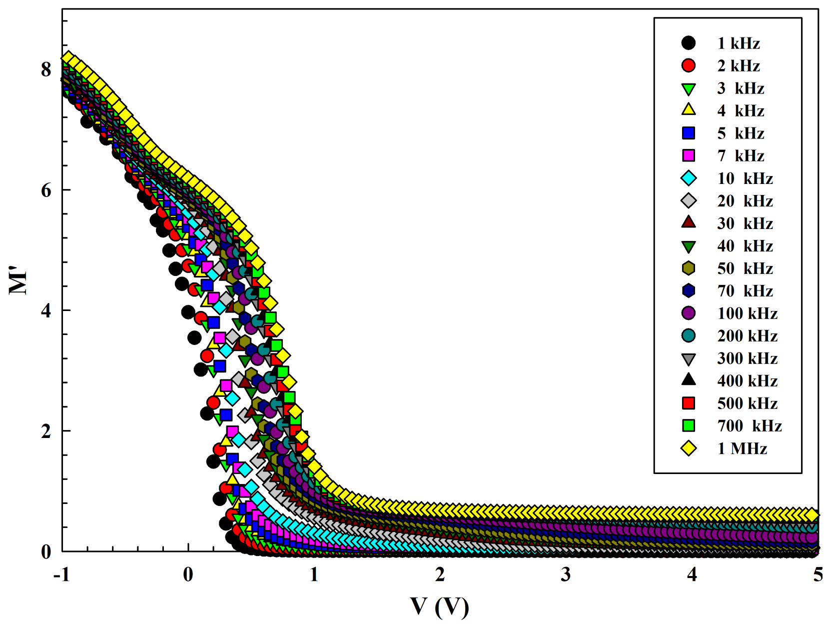

Figure 6. M′-V plot for Al/Mg_2Si/p-Si SD in a wide frequency range.

The conductivity properties and load storage capability of the structure can be examined using the AC electrical conductivity (σ_{AC}) given in Eq. 5 [40,41].

$$\sigma_{AC} = \omega C \left(\tan\delta\right)\left(\frac{d_i}{A}\right) = \omega\varepsilon_0\varepsilon''. \tag{5}$$

According to Eq. (5), σ_{AC} only depends on ε". Figure 8 shows the σ_{AC}-V plot of Al/Mg_2Si/p-Si SD in a wide frequency range. As shown in Figure 8, σ_{AC} is independent of frequency in the inversion and accumulation region and it takes a constant value in these regions. As the frequency increases, the value of σ_{AC} increases due to the decrease of the interface polarization, especially in depletion and accumulation regions. This increase causes an increase in eddy current. Such phenomena can be explained by a gradual decrease in series resistance (R_s) of the structure with increasing frequency [42–44]. In other words, the energy loss increases due to the increasing eddy currents. As the electrical conductivity increases, the value of tanδ also increases. The increasing σ_{AC} values are the result of ε", especially at high frequencies. In recently, similar results have been reported in the literature by various workers [37, 45–48].

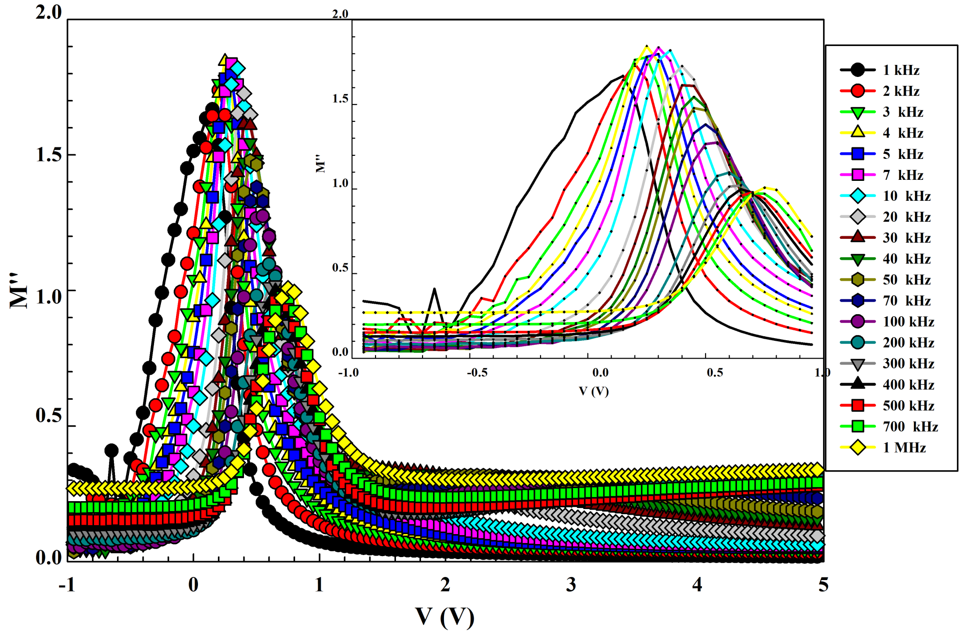

Figure 7. M$''$-V plot for Al/Mg_2Si/p-Si SD in a wide frequency range.

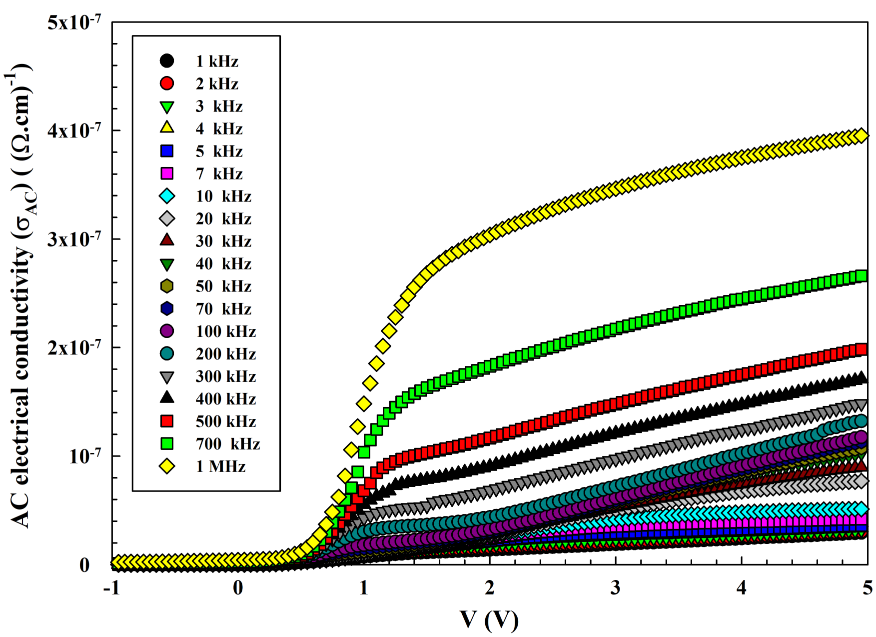

Figure 8. σ_{AC}-V plot for Al/Mg_2Si/p-Si SD in a wide frequency range.

4. Discussion

The complex dielectric permittivity ($\varepsilon^*=\varepsilon'-j\varepsilon''$), dielectric loss tangent ($\tan\delta$), the complex electric modulus ($M^*=M'+jM''$) of the Al/Mg_2Si/p-SiSD and its AC electrical conductivity (σ_{AC}) were calculated using the admittance measurements including measured capacitance and conductance data in a wide range from 1 kHz to 1 MHz. The variation of the frequency-dependent dielectric properties mainly depends on the electric dipole polarization, the interface polarization and the density distribution of the N_{ss}. Additionally, the values of ε', ε'', tanδ, M$'$ and M$''$ for the Al/Mg_2Si/p-Si SD were found as 0.756, 0.425, 0.562, 1.005 and 0.565 for 1 MHz at +5 V bias, respectively. The ε' is associated with interfacial and directional polarization while ε"is associated with transmission loss. The variation in values of ε', ε" and tanδ was attributed to the surface states, interfacial polarization and the decrease of C and G with increasing frequencies. N_{ss} follows the alternating signal especially at low or intermediate frequencies and affects the capacitance and conductivity values. The tanδ has a peak at low frequencies and this peak decreases with increasing frequency. This decrease was attributed to the inability of the hopping electrons to follow the external ac signal, with the dipole and surface polarizations reaching a constant value at high frequencies. The maximum value of the M$'$ at high frequencies is due to the frequency sensitivity of the dielectric relaxation mechanisms. The peak behavior of M$''$ in the depletion region has been attributed to the distribution of N_{ss} ingrained at the junction of the Mg_2Si and the p-Si and the MWt interface polarization. The increase in σ_{AC} with increasing frequency only contributes to the dielectric loss. Besides, the lost current caused by this increase increases the tanδ. This situation has been explained as the R_s decreases gradually with the increase in frequency. The obtained results showed that all-dielectric parameters (ε', ε", tanδ, M$'$, M$''$ and σ_{AC}) of the fabricated Al/Mg_2Si/p-Si SD depend on extreme frequency. Additionally, experimental results showed that the Mg_2Si, which is coated between the metal and semiconductor interface via spin coating method, can be used for more electronic charge storage instead of conventionally used dielectric materials (SnO_2, SiO_2).

References

[1] Popescu M, Bunget I. Physics of Solid Dielectrics. Amsterdam, Netherlands: Elsevier, 1984.

[2] Kwan CK. Dielectric Phenomena in Solids. Amsterdam, Netherlands: Elsevier, 2004.

[3] Chelkowski A. Dielectric Physics. Amsterdam, Netherlands: Elsevier, 1980.

[4] Lu L, Lai MO, Hoe ML. Formation of nanocrystalline Mg_2Si and Mg_2Si dispersion strengthened Mg-Al alloy by mechanical alloying. Nanostructured Materials 1998; 10 4: 551-563. doi: 10.1016/S0965-97739800102-0

[5] Mondolfo LF. Aluminum Alloys: Structure and Properties. London, UK: ButterWorth, 1976.

[6] Tani J, Kido H. Thermoelectric properties of Bi-doped Mg_2Si semiconductors. Physica B: Condensed Matter 2005; 364 (1-4): 218-224. doi: 10.1016/j.physb.2005.04.017

[7] Roberts GA, Cairns EJ, Reimer JA. Magnesium silicide as a negative electrode material for lithium-ion batteries. Journal of Power Sources 2002; 110 2: 424-429. doi: 10.1016/S0378-77530200207-0

[8] Kim H, Choi J, Sohn HJ, Kang T. The insertion mechanism of lithium into Mg2Si anode material for Li-ion batteries. Journal of the Electrochemical Society 1999; 146 12: 4401-4405. doi: 10.1149/1.1392650

[9] Bux SK, Yeung MT, Toberer ES, Snyder GJ, Kaner RB et al. Mechanochemical synthesis and thermoelectric properties of high quality magnesium silicide. Journal of Materials Chemistry 2011; 21 33: 12259-12266. doi: 10.1039/C1JM10827A

[10] Bose S, Acharya HN, Banerjee HD. Electrocal, thermal, thermoelectric and related properties of magnesium silicide semiconductor prepared from rice husk. Journal of Materials Science 1993; 28 20: 5461-5468. doi: 10.1007/BF00367816

[11] El-Amir Ahmed AM, Ohsawa T, Nabatame T, Ohi A, Wada Y et al. Ecofriendly Mg_2Si-based photodiode for short-wavelength IR sensing. Materials Science in Semiconductor Processing 2019; 91: 222-229. doi: 10.1016/j.mssp.2018.11.033

[12] Sekino K, Midonoya M, Udono H, Yamada Y. Preparation of Schottky contacts on-type Mg_2Si single crystalline substrate. Physics Procedia 2011; 11: 171-173. doi: 10.1016/j.phpro.2011.01.047

[13] Kato T, Sago Y, Fujiwara H. Optoelectronic properties of Mg_2Si semiconducting layers with high absorption coefficients. Journal of Applied Physics 2011; 110: 063723. doi: 10.1063/1.3642965

[14] Lenčéš Z, Hirao K, Šajgalík P, Hoffmann M. Thermodynamic and dielectric properties of $MgSiN_2$ ceramics. Key Engineering Materials 2006; 317-318: 857-860. doi: 10.4028/www.scientific.net/KEM.317-318.857

[15] Fu Z, Ma J, Liu P, Li Y, Zhang X. Crystal structure and microwave dielectric properties of middle-temperature-sintered $Mg_2Si_{(1-x)}V_xO_4$ ceramics. Journal of Electroceramics 2016; 36: 82-86. doi: 10.1007/s10832-016-0020-7 v Hyun Kim S, Choi K-H, Lee H-M, Hwang D-H, Do L-M et al. Impedance spectroscopy of single- and double-layer polymer light-emitting diode. Journal of Applied Physics 2000; 87: 882. doi: 10.1063/1.371956

[16] Saghrouni H, Jomni S, Belgacem W, Hamdaoui N, Beji L. Physical and electrical characteristics of metal/Dy_2O_3/p-GaAs structure. Physica B: Condensed Matter 2014; 444: 58-64. doi: 10.1016/j.physb.2014.03.030

[17] Nicollian EH, Brews JR. MOS (Metal Oxide Semiconductor) Physics and Technology. New York, NY, USA: John Wiley & Sons, 1982, pp. 257-264.

[18] Kınacı B, The temperature dependent negative dielectric constant phenomena of Au/n–GaAs structure with CZO interfacial layer. Journal of Materials Science: Materials in Electronics 2021; 32: 5928-5935. doi: 10.1007/s10854-021-05313-x

[19] Koçyiğit A, Orak İ, Türüt A. Temperature dependent dielectric properties of Au/ZnO/n-Si heterojuntion. Materials Research Express 2018; 5 3: 035906. doi: 10.1088/2053-1591/aab2e3

[20] Orak İ, Karabulut A. Frequency and voltage dependence of electrical conductivity, complex electric modulus, and dielectric properties of Al/Alq3/p-Si structure. Turkish Journal of Physics 2020; 44 1: 85-94. doi: 10.3906/fiz-1907-21

[21] Sevgili Ö, Azizian-Kalandaragh Y, Altındal Ş. Frequency and voltage dependence of electrical and dielectric properties in metal-interfacial layer-semiconductor (MIS) type structures. Physica B: Condensed Matter 2020; 587: 412122. doi: 10.1016/j.physb.2020.412122

[22] Yücedağ İ, Altındal Ş, Tataroğlu A. On the profile of frequency dependent series resistance and dielectric constant in MIS structure. Microelectronic Engineering 2007; 84 1: 180-186. doi: 10.1016/j.mee.2006.10.071

[23] Demirezen S. Frequency- and voltage-dependent dielectric properties and electrical conductivity of Au/PVA (Bi-doped)/n-Si Schottky barrier diodes at room temperature. Applied Physics A: Materials Science and Processing 2013; 112 4: 827-833. doi: 10.1007/s00339-013-7605-7

[24] Tataroğlu A, Yıldırım M, Baran HM. Dielectric characteristics of gamma irradiated Au/SnO_2/n-Si/Au (MOS) capacitor. Materials Science in Semiconductor Processing 2014; 28: 89-93. doi: 10.1016/j.mssp.2014.06.053

[25] Pochard I, Frykstrand S, Ahlström O, Forsgren J, Strømme M. Water and ion transport in ultra-adsorbing porous magnesium carbonate studied by dielectric spectroscopy. Journal of Applied Physics 2014; 115 4: 044306. doi: 10.1063/1.4860276

[26] Prabakar K, Narayandass SK, Mangalaraj D. Dielectric properties of $Cd_{0.6}Zn_{0.4}Te$ thin films. Physica Status Solidi (A) Applied Research 2003; 199 3: 507-514. doi: 10.1002/pssa.200306628

[27] Fouad SS, Sakr GB, Yahia IS, Abdel-Basset DM, Yakuphanoglu F. Capacitance and conductance characterization of nano-$ZnGa_2Te_4$/n-Si diode. Materials Research Bulletin 2014; 49: 369-383. doi: 10.1016/j.materresbull.2013.08.065

[28] Büyükbaş-Ulaşan A, Tataroğlu A. Effects of temperature on dielectric parameters of metal-oxide-semiconductor capacitor with thermal oxide layer. Journal of Nanoelectronics and Optoelectronics 2015; 10: 675-679. doi: 10.1166/jno.2015.1824

[29] Cherif A, Jomni S, Belgacem W, Elghoul N, Khirouni K et al. The temperature dependence on the electrical properties of dysprosium oxide deposited on p-Si substrate. Materials Science in Semiconductor Processing 2015; 29: 143-149. doi: 10.1016/j.mssp.2014.01.031

[30] Shukla N, Kumar V, Dwivedi DK. Dependence of dielectric parameters and A.C. conductivity on frequency and temperature in bulk $Se_{90}Cd_8In_2$ glassy alloy. Journal of Non-Oxide Glasses 2016; 8 (2): 47-57.

[31] Karabulut A, Türüt A, Karataş Ş. The electrical and dielectric properties of the Au/Ti/HfO2/n-GaAs structures. Journal of Molecular Structure 2018; 1157: 513-518. doi: 10.1016/j.molstruc.2017.12.087
[33] Shiwakoti N, Bobby A, Antony B, Asokan K. Interface state density and dielectric properties of Au/n-GaP Schottky diode. Journal of Vacuum Science & Technology B 2016; 34 5: 051206. doi: 10.1116/1.4961907

[32] Wang Z, Zhou W, Dong L, Sui X, Cai H et al. Dielectric spectroscopy characterization of relaxation process in Ni/epoxy composites. Journal of Alloys and Compounds 2016; 682: 738-745. doi: 10.1016/j.jallcom.2016.05.025

[33] Özen Y. Detailed consideration of electrical and dielectric properties of Au/Ni/n-Si MS structure in a wide frequency range. Silicon 2020. doi: 10.1007/s12633-020-00656-2

[34] Coşkun M, Polat Ö, Coşkun FM, Durmuş Z, Çağlar M et al. The electrical modulus and other dielectric properties by the impedance spectroscopy of $LaCrO_3$ and $LaCr_{0.90}Ir_{0.10}O_3$ perovskites. RSC Advances 2018; 8: 4634-4648. doi: 10.1039/C7RA13261A

[35] Azizian-Kalandaragh Y, Yücedağ İ, Ersöz Demir G, Altındal Ş. Investigation of the variation of dielectric properties by applying frequency and voltage to Al/(CdS-PVA)/p-Si structures. Journal of Molecular Structure 2021; 1224 (1-5): 129325. doi: 10.1016/j.molstruc.2020.129325

[36] Sevgili Ö, Taşçıoğlu İ, Boughdachi S, Azizian-Kalandaragh Y, Altındal Ş. Examination of dielectric response of Au/HgS-PVA/n-Si (MPS) structure by impedance spectroscopy method. Physica B: Condensed Matter 2019; 566: 125-135. doi: 10.1016/j.physb.2019.04.029

[37] Tataroğlu A, Altındal Ş, Bülbül MM. Temperature and frequency dependent electrical and dielectric properties of Al/SiO_2/p-Si (MOS) structure. Microelectronic Engineering 2005; 81 1: 140-149. doi: 10.1016/j.mee.2005.04.008

[38] Karabulut A. Dielectric characterization of Si-based heterojunction with TiO_2 interfacial layer. Journal of the Institute of Science and Technology 2018; 8 3: 119-129. doi: 10.21597/jist.418869

[39] Tecimer H. On the frequency–voltage dependent electrical and dielectric profiles of the Al/(Zn-PVA)/p-Si structures. Journal of Materials Science: Materials in Electronics 2018; 29: 20141-20145. doi: 10.1007/s10854-018-0146-2

[40] Dubey AK, Singh P, Singh S, Kumar D, Parkash O. Charge compensation, electrical and dielectric behavior of lanthanum doped $CaCu_3Ti_4O_{12}$. Journal of Alloys and Compounds 2011; 509 9: 3899-3906. doi: 10.1016/j.jallcom.2010.12.156

[41] Tataroğlu A, Yücedağ İ, Altındal Ş. Dielectric properties and ac electrical conductivity studies of MIS type Schottky diodes at high temperatures. Microelectronic Engineering 2008; 85 7: 1518-1523. doi: 10.1016/j.mee.2008.02.005

[42] Ertuğrul R, Tataroğlu A. Influence of temperature and frequency on dielectric permittivity and ac conductivity of Au/SnO_2/n-Si (MOS) structures. Chinese Physics Letters 2012; 29 7: 077304. doi: 10.1088/0256-307X/29/7/077304

[43] Badali Y, Altindal Ş, Uslu İ. Dielectric properties, electrical modulus and current transport mechanisms of Au/ZnO/n-Si structures. Progress in Natural Science: Materials International 2018; 28 3: 325-331. doi: 10.1016/j.pnsc.2018.05.003

[44] Karadaş S, Altındal Yerişkin S, Balbaşı M, Azizian-Kalandaragh Y. Complex dielectric, complex electric modulus, and electrical conductivity in Al/(Graphene-PVA)/p-Si (metal-polymer-semiconductor) structures. Journal of Physics and Chemistry of Solids 2021; 148: 109740. doi: 10.1016/j.jpcs.2020.109740

[45] Altındal Yerişkin S, Ersöz Demir G, Yücedağ İ. On the frequency-voltage dependence profile of complex dielectric, complex electric modulus and electrical conductivity in Al/ZnO/p-GaAs type structure at room temperature. Journal of Nanoelectronics and Optoelectronics 2019; 14 8: 1126-1132. doi: 10.1166/jno.2019.2623

[46] Kaya A, Vural Ö, Tecimer H, Demirezen S, Altındal Ş. Frequency and voltage dependence of dielectric properties and electric modulus in Au/PVC+TCNQ/p-Si structure at room temperature. Current Applied Physics 2014; 14: 322-330. doi: doi: 10.1016/j.cap.2013.12.005